analytical chemistry

Technical Note

pubs.acs.org/ac

# Implementation of Molecularly Imprinted Polymer Beads for Surface Enhanced Raman Detection

Tripta Kamra,[†,‡,§] Tongchang Zhou,[†] Lars Montelius,[§,∥] Joachim Schnadt,[‡] and Lei Ye*[,†]

[†]Division of Pure & Applied Biochemistry, Department of Chemistry, Lund University, Box 124, 221 00 Lund, Sweden
[‡]Division of Synchrotron Radiation Research, Department of Physics, Lund University, Box 118, 221 00 Lund, Sweden
[§]Division of Solid State Physics, Department of Physics, Lund University, Box 118, 221 00 Lund, Sweden

Supporting Information

**ABSTRACT:** Molecularly imprinted polymers (MIPs) have a predesigned molecular recognition capability that can be used to build robust chemical sensors. MIP-based chemical sensors allow label-free detection and are particularly interesting due to their simple operation. In this work we report the use of thiol-terminated MIP microspheres to construct surfaces for detection of a model organic analyte, nicotine, by surface enhanced Raman scattering (SERS). The nicotine-imprinted microspheres are synthesized by RAFT precipitation polymerization and converted into thiol-terminated microspheres through aminolysis. The thiol groups on the MIP surface allow the microspheres to be immobilized on a gold-coated substrate. Three different strategies are investigated to achieve surface enhanced Raman scattering in the vicinity of the imprinted sites: (1) direct sputtering of gold nanoparticles, (2) immobilization of gold colloids through the MIP's thiol groups, and (3) trapping of the MIP microspheres in a patterned SERS substrate. For the first time we show that large MIP microspheres can be turned into selective SERS surfaces through the three different approaches of assembly. The MIP-based sensing surfaces are used to detect nicotine to demonstrate the proof of concept. As synthesis and surface functionalization of MIP microspheres and nanoparticles are well established, the methods reported in this work are handy and efficient for constructing label-free chemical sensors, in particular for those based on SERS detection.

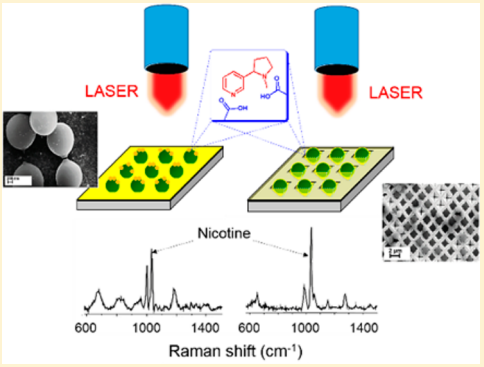


In recent years there has been increasing interest for the detection of bioactive molecules in complex samples such as drugs,[1] proteins, and nucleic acids.[2] Here, chemical sensors and biosensors play an important role due to their handy operation. In biosensors, the recognition elements may be obtained from different biological systems, e.g., antibodies and aptamers that are particularly useful for the detection of biomacromolecules. These biological systems are, however, not particularly successful in recognizing low molecular weight analytes and, moreover, they have only limited stability. For small molecule detection molecularly imprinted polymers (MIPs) have shown great promise, and MIP-based chemical sensors for low molecular weight compounds have been reported in numerous publications.[3−6] In MIPs, the molecular recognition sites are created in cross-linked polymers with high mechanical and chemical stability, providing MIP-based chemical sensors with outstanding durability. Combining the molecular selectivity of the MIPs with a spectroscopic transducer has been proven very powerful for the detection of organic molecules in complex samples, thanks to the synergy of selective molecular binding from the MIP and the fingerprint identification offered by the spectroscopic transducer. Previously, MIPs have been combined with IR evanescent wave spectroscopy[7] and a surface enhanced Raman scattering (SERS) transducer[8] to detect small organic analytes. Among the different optical sensing constructs, MIP sensors using SERS detection have become the most popular one,[9−12] and portable Raman instruments are now available from many commercial vendors, with which detection can be carried out directly on both solid and liquid samples.

In Raman spectroscopy, the analyte molecules interact with a monochromatic incident light and scatter photons of different wavelengths. The Raman signal from inelastic scattering, although characteristic for each analyte, is often very weak and difficult to detect. This problem of low sensitivity can be solved by depositing analytical samples on a roughened noble metal surface (e.g., silver or gold)[13−15] or on a metal-coated rough porous surface[16−18] that can generate localized surface plasmons upon light irradiation. The plasmon resonance is the basis for SERS.[19] When the analyte molecule is located close enough to the metal surface, the SERS signal can be increased by many orders of magnitude in comparison to ordinary Raman spectroscopy.[20]

One of the most important challenges in building MIP-based SERS sensors is to make sure that the MIPs carrying the molecular recognition sites are integrated intimately with the

**Received:** February 26, 2015
**Accepted:** April 21, 2015
**Published:** April 21, 2015

  

DOI: 10.1021/acs.analchem.5b00774
*Anal. Chem.* 2015, 87, 5056−5061

SERS-active surface, so that the surface can effectively enhance the otherwise weak Raman signal. In most previous studies, the MIP components were prepared in situ on Raman-active surfaces.[21,22] The in situ preparation is limited by the required quantity of noble metals, which is expensive and difficult to use on a large scale.

In this work we report three new approaches that allow premade MIP microspheres to be integrated into SERS sensors. The nicotine-imprinted microspheres are synthesized by reversible addition−fragmentation chain transfer (RAFT) precipitation polymerization and are decorated with terminal thiol groups, which allow the microspheres to be easily immobilized on a gold substrate. SERS was achieved by locating the SERS active material in the vicinity of the imprinted sites through (1) direct sputtering of gold nanoparticles on the MIP microspheres, (2) immobilization of gold colloids through the thiol groups of the MIPs, and (3) trapping MIP microspheres on a commercial SERS-active substrate. Using these methods we can integrate optimized MIP microspheres into SERS sensors without complicated chemical reaction steps. Although we demonstrate the concept using MIP microspheres, the methods are also applicable to MIP nanoparticles bearing other surface thiol groups, and therefore the methods are generally useful for building up MIP-based SERS sensors.

## EXPERIMENTAL SECTION

**Materials.** Klarite surfaces were purchased from Renishaw Diagnostics (D3 Technologies Ltd.). These SERS active substrates are comprised of Au coated inverse pyramidal grids of 1.5 × 1.5 $\mu m^2$ area and a depth of 1 $\mu$m.[23−25] Gold colloids (20 nm, citrate stabilized and suspended in ethanol, particle concentration 7 × $10^{11}$ $mL^{-1}$) were purchased from Sigma-Aldrich.

Molecularly imprinted polymer microspheres bearing thiol groups (MIP-SH) were synthesized using nicotine as a template by RAFT precipitation polymerization.[26] For comparison, nonimprinted polymer microspheres bearing thiol groups (NIP-SH) were also synthesized under the same condition except for the omission of the template.

**Preparation of Au-Coated Wafer.** The Au-coated substrate was prepared by evaporating 200 nm Au onto a 2 in. clean silicon (Si) wafer precoated with a 20 nm titanium adhesion layer. The Au-coated substrate was then cut into surfaces of 6 × 6 $mm^2$ size, which were cleaned by sonication in acetone for a few minutes followed by a rinse in ethanol. The surfaces were then washed in distilled water, dried under a nitrogen flow, and stored in a vacuum desiccator.

**Immobilization of Polymer Microspheres.** MIP-SH and NIP-SH microspheres were suspended in acetonitrile (2 mg $mL^{-1}$) and sonicated to give a homogeneous particle suspension. The Au-coated wafers were submerged in the particle suspension (1 mL) and kept there for 12−16 h, and the commercial Klarite substrate was overflown with 100 $\mu$L of the particle suspension for 4−5 times. This treatment allowed the polymer microspheres to bind to the Au surfaces. The loosely adhered particles were removed by rinsing the surfaces briefly in acetonitrile: the Au-coated wafers covered by the microspheres were dipped in 1 mL of acetonitrile two times, and the Klarite substrate loaded with the microspheres was overflown with 100 $\mu$L of acetonitrile two times. The obtained surfaces were dried in a desiccator until further use.

**Procedure of Nicotine Analysis Using Different SERS Substrates.** *Activation of the MIP Surface by Sputtered Au Deposition.* The surface-immobilized polymer particles were first sputter-coated with 5 nm gold and then incubated in different nicotine solutions in acetonitrile for 3 h. The surfaces were rinsed briefly in acetonitrile and dried before the Raman spectra were collected.

*Activation of the MIP Surface by Immobilization of Au Nanoparticles.* The surface-immobilized polymer particles were first incubated in different nicotine solutions in acetonitrile for 3 h. The surfaces were then rinsed briefly in acetonitrile, transferred into the Au colloid solution, and kept there for 12 h. Finally, the surfaces were rinsed with ethanol and dried before the Raman spectra were collected.

*Activation of MIP Using Patterned SERS Substrate.* The particle-loaded Klarite substrates were incubated in nicotine solution in acetonitrile for 3 h. The surfaces were rinsed briefly with acetonitrile and dried before the Raman spectra were collected.

## RESULTS AND DISCUSSION

In a previous work, we synthesized nicotine-imprinted polymer microspheres using RAFT precipitation polymerization.[26] The MIP microspheres displayed a narrow size distribution and high molecular binding selectivity for nicotine. In addition, we demonstrated that the MIP beads could be converted into thiol-functionalized particles through a simple aminolysis reaction. The thiol groups introduced to the surface of the MIP microspheres made it possible to introduce new function to the molecularly imprinted material, e.g., by conjugating fluorescent dyes to the particles.[26] Considering the potent thiol−gold interaction, we envisage that the surface thiol groups should allow the MIP-SH beads to be firmly anchored to gold surfaces, thereby offering a convenient means to immobilizing the MIP particles on a gold coated surface as well as to accumulate gold colloids on the MIP particles through their abundant thiol groups. On the basis of these considerations, we designed three different approaches to construct MIP-based SERS substrates for label-free detection of the model analyte, nicotine. To achieve SERS signal from the bound nicotine molecules, it is critical that we can manage to locate the molecularly imprinted sites to be close enough to a Raman active surface, e.g., a roughened Au substrate or Au nanoparticles.[27]

**Immobilization of MIP-SH Microspheres through Thiol−Au Bonding.** To prepare nicotine-selective substrates that can be conveniently used in optical sensing, we first investigated the possibility of immobilizing the MIP-SH microspheres through their surface thiol groups on a Au-coated silicon substrate. From Figure 1A it is evident that a high density of the MIP-SH microspheres is fixed on the Au surface and that the particles cover the Au surface rather homogeneously with no significant aggregation. The number of the MIP-SH beads immobilized on a 6 × 6 $mm^2$ surface is estimated to be approximately 3 × $10^9$. For the control surface made from the NIP-SH microspheres, the polymer beads deposited on the Au surface are larger than the MIP-SH particles (Figure 1B), which is in agreement with the different particle sizes that we observed in our previous work.[26] Nevertheless, a high density of the NIP-SH particle coating on the surface was achieved due to the potent thiol−Au bonding. To prove that the Au surface is necessary to achieve a stable immobilization of the thiol-functionalized particles, we


DOI: 10.1021/acs.analchem.5b00774
Anal. Chem. 2015, 87, 5056−5061

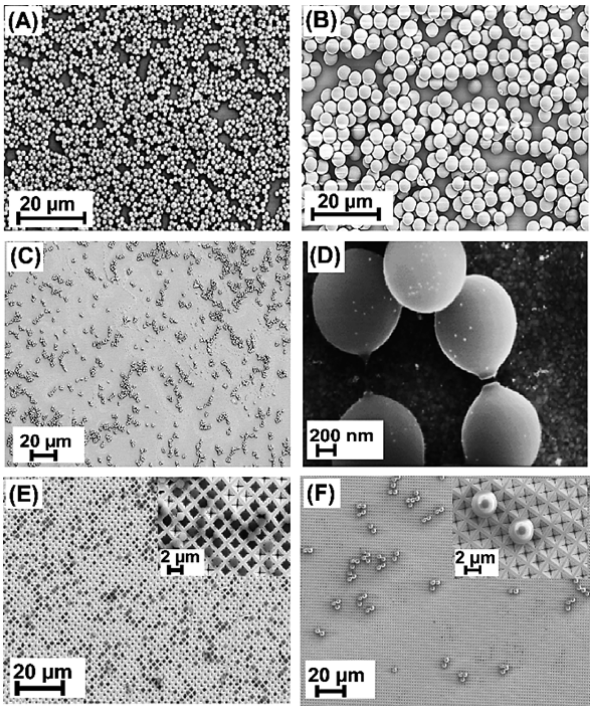


**Figure 1.** SEM images of (A) MIP-SH deposited on a Au surface, (B) NIP-SH deposited on a Au surface, (C) MIP-SH deposited on Si wafer, (D) MIP-SH deposited on a Au surface followed by deposition of 20 nm Au colloids, (E) Klarite surface after loading the MIP-SH, and (F) Klarite surface loaded with NIP-SH.

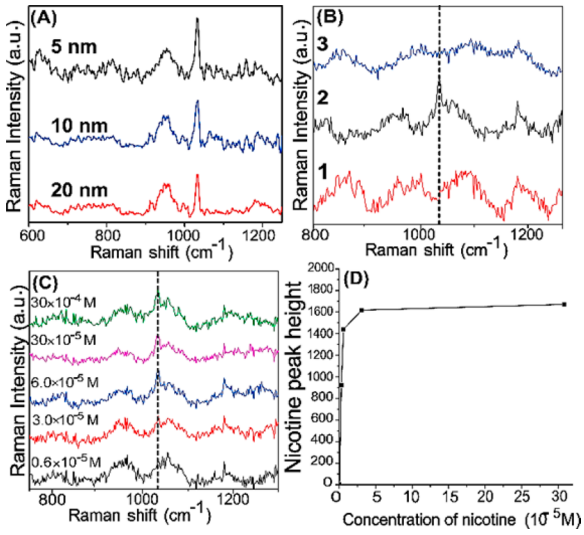


**Figure 2.** (A) Raman signal detected from a MIP-SH surface sputter-coated with Au of different thickness. (B) Raman spectra collected from (1) a MIP surface after Au sputtering, (2) a MIP surface after Au sputtering and exposure to $6 \times 10^{-5}$ M nicotine, (3) a NIP surface after Au sputtering and exposure to $6 \times 10^{-5}$ M nicotine. (C) Raman spectra collected from an activated MIP surface after exposure to increased concentrations of nicotine solutions. (D) Plot of Raman intensity vs nicotine concentration, obtained using the activated MIP surface.

treated a clean Si wafer with the same particle suspension and inspected the surface with SEM. As shown in Figure 1C, the number of the immobilized particles ($2 \times 10^8$) was reduced significantly in comparison with the Au-coated surface, which indicates that the thiol–Au interaction indeed is critical for obtaining reliable particle immobilization.

**Activation of Sensing Surface by Sputter Coating of a Au Layer.** In a preliminary experiment, we exposed the Au surface on which MIP-SH particles had been immobilized to a nicotine solution and then collected the Raman signal. As expected, no nicotine signal could be detected due to the lack of Raman "hot spots" on the sensing surface (data not shown). To activate the sensing surface, we first sputter-coated the MIP-SH-covered surface with a thin layer of Au using a standard laboratory coater. As reported by Fu et al.,[28] sputtering of Au granules of a particular thickness generates an enhanced Raman signal. Here we used a short sputtering time to make sure that the sputtered Au (5 nm) did not form a continuous film (Figure S1 in the Supporting Information), which otherwise would completely block the surface of the MIP-SH beads.[29] After Au sputtering, the activated MIP-SH surface was exposed to a nicotine solution and then analyzed by Raman spectroscopy. As shown in Figure 2A, when the MIP-SH surface sputter-coated with 5 nm Au was exposed to a nicotine solution ($6 \times 10^{-5}$ M), it generated the strongest Raman signal at 1034 $cm^{-1}$. In Figure 2B, for the activated surface alone (i.e., in the absence of the template) no nicotine signal was detected, whereas after nicotine binding a nicotine-characteristic Raman band at 1034 $cm^{-1}$ (indicated by the dotted line) became evident.[30] Under the same conditions, the NIP-SH surface activated by Au sputter coating did not generate any nicotine signal, in line with the lack of the nicotine binding sites in the NIP-SH particles. On the basis of these results, we conclude that the simple method of Au sputter coating on MIP-SH indeed turned the nicotine selective surface to be Raman active, and it was possible to detect the selective nicotine binding via the activated "hot spots".[31] Obviously, the MIP-SH beads were able to bind nicotine in spite of the sputtered Au deposited on their surface. Although the nicotine signal detected in this set up is relatively weak, the method of Au sputtering to activate MIP for Raman measurement is very easy to carry out and is much cheaper than using commercial SERS substrates.

Activation by Au sputter coating allows Raman "hot spots" to be generated on the surface of the MIP-SH microspheres. In this manner only the binding sites close to the particle surface can be utilized to give effective signal response, because the nicotine molecules bound in the interior of the particles are "invisible". Since the number of "visible" binding sites is limited, it is likely that these sites will be saturated at high nicotine concentration. Indeed, Figure 2C,D shows that when the concentration of nicotine exceeds $30 \times 10^{-5}$ M, the detected Raman signal intensity does not increase further.

**Activation of Sensing Surface by Immobilizing Au Nanoparticles.** Instead of Au sputtering, we considered it possible to conjugate premade gold colloidal particles on the surface of the MIP-SH sample through binding to the abundant thiol groups. Compared to Au sputter coating, this procedure can be carried out in solution using commercially available gold colloids. Here we used 20 nm gold nanoparticles protected by tannic acid/citrate ligands. Immobilization of the Au nanoparticles was done by simply dipping the immobilized MIP-SH surface into the commercial gold solution. The high-resolution SEM in Figure 1D shows clearly the 20 nm gold nanoparticles (as bright dots) that are fixed on the MIP surface. The gold nanoparticles seem to distribute randomly on the MIP particles and have a relatively low surface coverage. When tested with a nicotine solution, this activated surface generated a very intense


DOI: 10.1021/acs.analchem.5b00774
Anal. Chem. 2015, 87, 5056–5061

Raman band at 1034 $cm^{-1}$ (Figure 3A). The enhancement of the Raman signal is attributed to the plasmonic coupling

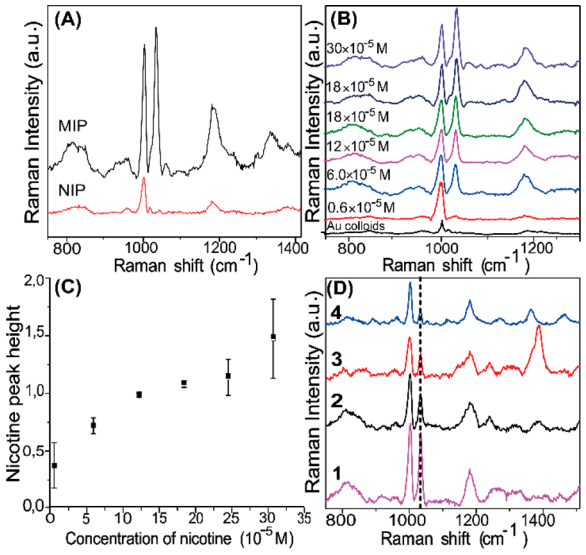


**Figure 3.** (A) Raman spectra of 30 × $10^{-5}$ M nicotine obtained from MIP-SH and NIP-SH surfaces after deposition of Au colloids. (B) Raman spectra of nicotine obtained from the MIP-SH surface after deposition of Au colloids. (C) Relative intensity of Raman band of nicotine at 1034 $cm^{-1}$ normalized against the band at 1004 $cm^{-1}$. (D) Raman spectra of (1) 6 × $10^{-5}$ M nicotine, (2) 6 × $10^{-5}$ M nicotine mixed with 3.4 × $10^{-5}$ M propranolol, (3) 6 × $10^{-5}$ M nicotine mixed with 34 × $10^{-5}$ M propranolol, (4) 6 × $10^{-5}$ M nicotine mixed with 34 × $10^{-5}$ M Rhodamine B. The spectra were collected from the MIP surface after deposition of Au colloids.

between the surface-bonded Au colloids combined with the enriched nicotine molecules through their specific binding to the MIP-SH microspheres resulting in local electromagnetic field enhancements.[32,33] The argument is further supported by the results for the NIP-SH surface, for which no clear nicotine signal is visible under the same conditions. Interestingly, the Au colloids themselves produced a strong Raman band at 1004 $cm^{-1}$, which can be explained as a result of the phenol structure in the tannic acid.[34] Using this intrinsic Raman signal of Au colloids as an internal standard, we were able to establish a dose–response curve for the nicotine measurement (Figure 3B,C). In Figure 3C, the signal was recorded at three different spots on the same surface and the error bar shows the standard deviation from each surface.

To confirm that the immobilized MIP-SH microspheres maintain their selectivity under the measurement condition, we also measured the Raman spectra of nicotine mixed with different amounts of propranolol. The surfaces were incubated in nicotine (6 × $10^{-5}$ M) spiked with different quantities of propranolol (3.4 × $10^{-5}$ M and 34 × $10^{-5}$ M) and Rhodamine B (34 × $10^{-5}$ M) before collecting the Raman spectra. As shown in Figure 3D, although addition of propranolol caused the nicotine signal to decrease slightly, the characteristic nicotine band at 1034 $cm^{-1}$ is much higher than the propranolol signal at 1385 $cm^{-1}$.[35] Even in the presence of excess Rhodamine B (a basic and Raman active dye having a characteristic band at 1360 $cm^{-1}$),[36] the nicotine signal at 1034 $cm^{-1}$ is still clearly visible. These results are clear indications of the binding selectivity of the MIP-SH beads toward nicotine, which makes nicotine more easily detected via SERS. We should note that in this approach the MIP-SH coated surface was first dipped in the analyte solution, then rinsed briefly in water, before it was treated with the commercial gold solution. The reason that this procedure resulted in an improved Raman signal can be explained as follows: binding of the basic nicotine molecules to MIP-SH could neutralize the otherwise negatively charged polymer surface, making the tannic acid-protected gold colloids easier to reach the thiol groups on the polymer surface.[37]

**Activation of MIP Using Patterned SERS Substrate.** Besides using in-house prepared SERS surfaces, we also investigated if the uniform MIP-SH microspheres can be directly applied onto a commercial SERS substrate for Raman sensing. The Klarite substrate we selected consists of uniform 1.5 × 1.5 $\mu m^2$ etched pyramid cavities coated with roughened gold (Figure S2B in the Supporting Information). The size of the individual cavities on the Klarite surface was considered suitable to hold the MIP-SH beads in place, so that the bead-loaded cavities can produce a detectable Raman signal. Figure 1E,F shows the SEM images of a Klarite substrate after loading of the MIP-SH and NIP-SH microspheres. From Figure 1E, it is clear that the MIP-SH beads (1.3–2 $\mu m$) fit snugly in the surface cavities of the Klarite substrate with no severe aggregation. In contrast, the NIP-SH beads (~4.3 $\mu m$) are too large to fit in the surface cavities, making the NIP-SH beads more difficult to be fixed on the Klarite substrate (Figure 1F). Moreover, we observed that the MIP-SH beads, after entering the patterned cavities, remain stable and can withstand repeated measurements. Although complete loading of the cavities requires further optimization or may require more sophisticated instrumentation (e.g., an inkjet printer),[38,39] we proceeded with the nonoptimized surface to see if it can be used directly for Raman measurement.

To study the Raman response of the MIP-loaded Klarite, we incubated the surface in a series of nicotine samples of increasing concentration (0.6–30 × $10^{-5}$ M) and performed the Raman measurement. To avoid large deviation caused by the noncomplete particle coverage, we used the intrinsic Raman band of the polymer at 1152 $cm^{-1}$ as an internal standard. Figure 4A shows Raman spectra of different nicotine samples obtained with the MIP-loaded Klarite substrate, and Figure 4B presents a dose–response curve for the normalized nicotine signal derived from Figure 4A. Figure 4C shows the Raman spectra of the Klarite substrates that have been loaded with the MIP-SH and NIP-SH spheres, before and after being exposed to a nicotine solution. Obviously, the nicotine signal detected from the MIP-SH-loaded Klarite is enabled by the combination of the selective molecular binding with the SERS-enabling surface. Despite the simple procedure used to prepare the SERS substrate, the Raman measurement based on the MIP-loaded Klarite surface displays a high sensitivity.

## ■ CONCLUSIONS

We investigated three approaches for implementing molecularly imprinted microspheres to realize SERS detection for small organic analytes. A common feature of these approaches is the use of surface thiol groups to immobilize MIP microspheres on a Au-coated surface to provide a selective molecular recognition layer. To make the molecular recognition layer become SERS active, Au sputter coating, colloidal gold deposition, and loading of MIP-SH beads onto a patterned SERS substrate were investigated. All of the three methods were successful in enabling MIP beads to detect nicotine via SERS measurements.


DOI: 10.1021/acs.analchem.5b00774
*Anal. Chem.* 2015, 87, 5056–5061

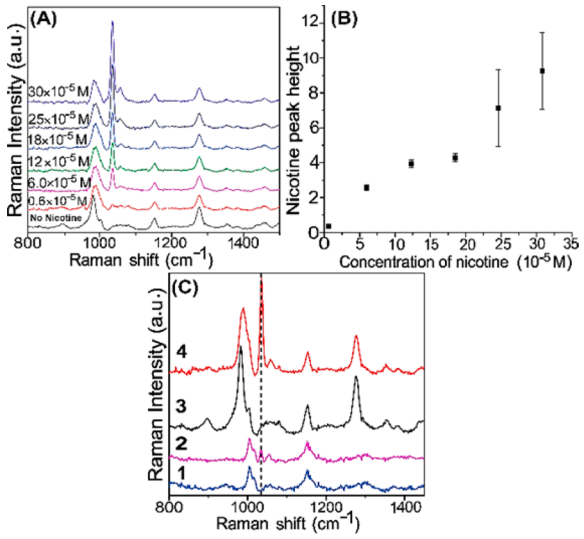


**Figure 4.** (A) Raman spectra of nicotine samples obtained from the MIP-SH-loaded Klarite substrate. (B) Dose−response curve of Raman intensity at 1034 $cm^{-1}$ normalized against the internal standard signal at 1152 $cm^{-1}$. (C) Raman spectra of (1) NIP-SH-loaded Klarite substrate, (2) NIP-SH-loaded Klarite substrate after exposure to $6 \times 10^{-5}$ M nicotine, (3) MIP-SH-loaded Klarite substrate, and (4) MIP-SH-loaded Klarite substrate after exposure to $6 \times 10^{-5}$ M nicotine.

The Au sputter coating method is the most cost-effective, but it resulted in a relatively weak signal only. The method of colloidal Au deposition took longer time for sample preparation; however, it produces a strong analytical signal. Loading the MIP-SH beads on the commercial Klarite substrate is the simplest approach, yet it is the most expensive method due to the high cost of the commercial substrate. Because of the use of the relatively large MIP microspheres, not all the molecular binding sites in the MIP have been utilized. Nevertheless, the present results show clearly that the proposed approaches are successful in enabling ordinary MIPs for detection of organic analytes using the SERS technique. We believe that by using smaller MIP nanoparticles in combination with better-controlled nanoparticle deposition, MIP-based SERS surfaces can be obtained with more precise control and the analytical performance of such sensing elements can be improved significantly to satisfy practical applications.

## ■ ASSOCIATED CONTENT

### Supporting Information

Synthesis of polymer microspheres, AFM, and additional SEM images. The Supporting Information is available free of charge on the ACS Publications website at DOI: 10.1021/acs.analchem.5b00774.

## ■ AUTHOR INFORMATION

### Corresponding Author

*E-mail: lei.ye@tbiokem.lth.se. Phone: +46 46 22 29560.

### Present Address

[‖]L.M.: International Iberian Nanotechnology Laboratory, Avenida Mestre José Veiga s/n, 4715-330 Braga, Portugal.

### Notes

The authors declare no competing financial interest.

## ■ ACKNOWLEDGMENTS

We are grateful for financial support from the European Commission via the Marie Curie Initial Training Network SMALL (Grant No. 238804), the Swedish Research Council FORMAS (Grant No. 212-2013-1350), and the Danish Council for Strategic Research (Project FENAMI, DSF-10-93456).

## ■ REFERENCES

(1) Pal, T.; Narayanan, V. A.; Stokes, D. L.; Vo-Dinh, T. *Anal. Chim. Acta* **1998**, *368*, 21−28.
(2) Ye, S.; Wu, Y.; Zhang, W.; Li, N.; Tang, B. *Chem. Commun.* **2014**, *50*, 9409−12.
(3) Zhang, Q.; Jing, L.; Wang, Y.; Zhang, J.; Ren, Y.; Wang, Y.; Wei, T.; Liedberg, B. *Anal. Biochem.* **2014**, *463*, 7−14.
(4) Kolarov, F.; Niedergall, K.; Bach, M.; Tovar, G. E. M.; Gauglitz, G. *Anal. Bioanal. Chem.* **2012**, *402*, 3245−3252.
(5) Walker, N. R.; Linman, M. J.; Timmers, M. M.; Dean, S. L.; Burkett, C. M.; Lloyd, J. A.; Keelor, J. D.; Baughman, B. M.; Edmiston, P. L. *Anal. Chim. Acta* **2007**, *593*, 82−91.
(6) Das, K.; Penelle, J.; Rotello, V. M. *Langmuir* **2003**, *19*, 3921−3925.
(7) Jakusch, M.; Janotta, M.; Mizaikoff, B.; Mosbach, K.; Haupt, K. *Anal. Chem.* **1999**, *71*, 4786−4791.
(8) Kostrewa, S.; Emgenbroich, M.; Klockow, D.; Wulff, G. *Macromol. Chem. Phys.* **2003**, *204*, 481−487.
(9) Kantarovich, K.; Tsarfati, I.; Gheber, L. A.; Haupt, K.; Bar, I. *Biosens. Bioelectron.* **2010**, *26*, 809−814.
(10) Bompart, M.; De Wilde, Y.; Haupt, K. *Adv. Mater.* **2010**, *22*, 2343−8.
(11) Liu, P.; Liu, R. Y.; Guan, G. J.; Jiang, C. L.; Wang, S. H.; Zhang, Z. P. *Analyst* **2011**, *136*, 4152−4158.
(12) Holthoff, E. L.; Stratis-Cullum, D. N.; Hankus, M. E. *Sensors* **2011**, *11*, 2700−2714.
(13) Zhang, Z.; Zhang, S.; Lin, M. *Analyst* **2014**, *139*, 2207−13.
(14) Xue, J.-Q.; Li, D.-W.; Qu, L.-L.; Long, Y.-T. *Anal. Chim. Acta* **2013**, *777*, 57−62.
(15) Chang, L.; Ding, Y.; Li, X. *Biosens. Bioelectron.* **2013**, *50*, 106−110.
(16) Ignat, T.; Kleps, I.; Miu, M.; Craciunoiu, F.; Bragaru, A.; Simion, M. *Proceedings of the International Semiconductor Conference, CAS*, October 13−15, 2008; pp 197−200.
(17) Ignat, T.; Munoz, R.; Irina, K.; Obieta, I.; Mihaela, M.; Simion, M.; Iovu, M. *Superlattices Microstruct.* **2009**, *46*, 451−460.
(18) Bompart, M.; Gheber, L. A.; De Wilde, Y.; Haupt, K. *Biosens. Bioelectron.* **2009**, *25*, 568−571.
(19) Moskovits, M. *J. Raman Spectrosc.* **2005**, *36*, 485−496.
(20) Tian, Z. Q. *J. Raman Spectrosc.* **2005**, *36*, 466−470.
(21) Chang, L.; Wu, S.; Chen, S.; Li, X. *J. Mater. Sci.* **2011**, *46*, 2024−2029.
(22) Guo, Z.; Chen, L.; Lv, H.; Yu, Z.; Zhao, B. *Anal. Methods* **2014**, *6*, 1627−1632.
(23) Hankus, M. E.; Stratis-Cullum, D. N.; Pellegrino, P. M. *Proc. SPIE* **2011**, 80997.
(24) Alexander, T. A. *Proc. SPIE* **2005**, 600703.
(25) Vernon, K. C.; Davis, T. J.; Scholes, F. H.; Gómez, D. E.; Lau, D. *J. Raman Spectrosc.* **2010**, *41*, 1106−1111.
(26) Zhou, T. C.; Jorgensen, L.; Mattebjerg, M. A.; Chronakis, I. S.; Ye, L. *RSC Adv.* **2014**, *4*, 30292−30299.
(27) Ko, H.; Singamaneni, S.; Tsukruk, V. V. *Small* **2008**, *4*, 1576−1599.
(28) Fu, C. Y.; Dinish, U. S.; Rautela, S.; Goh, D. W.; Olivo, M. *Proc. SPIE* **2011**, 82041O.
(29) Muzard, S.; Templier, C.; Delafond, J.; Girard, J. C.; Thiaudiere, D.; Pranevicius, L.; Galdikas, A. *Surf. Coat. Technol.* **1998**, *100−101*, 98−102.
(30) Barber, T. E.; List, M. S.; Haas, J. W.; Wachter, E. A. *Appl. Spectrosc.* **1994**, *48*, 1423−1427.



DOI: 10.1021/acs.analchem.5b00774
*Anal. Chem.* 2015, 87, 5056−5061

(31) Farcau, C.; Astilean, S. *J. Phys. Chem. C* **2010**, *114*, 11717−11722.
(32) Tao, C. A.; An, Q.; Zhu, W.; Yang, H.; Li, W.; Lin, C.; Xu, D.; Li, G. *Chem. Commun.* **2011**, *47*, 9867−9869.
(33) Ye, Y.; Liu, H.; Yang, L.; Liu, J. *Nanoscale* **2012**, *4*, 6442−6448.
(34) Evans, J. C. *Spectrochim. Acta* **1960**, *16*, 1382−1392.
(35) Levene, C.; Correa, E.; Blanch, E. W.; Goodacre, R. *Anal. Chem.* **2012**, *84*, 7899−905.
(36) Sun, C. H.; Wang, M. L.; Feng, Q.; Liu, W.; Xu, C. X. *Russ. J. Phys. Chem.* **2015**, *89*, 291−296.
(37) Alharbi, O.; Xu, Y.; Goodacre, R. *Analyst* **2014**, *139*, 4820−4827.
(38) Farrell, M. E.; Holthoff, E. L.; Pellegrino, P. M. *Appl. Spectrosc.* **2014**, *68*, 287−296.
(39) Emmons, E. D.; Farrell, M. E.; Holthoff, E. L.; Tripathi, A.; Green, N.; Moon, R. P.; Guicheteau, J. A.; Christesen, S. D.; Pellegrino, P. M.; Fountain, A. W., III *Appl. Spectrosc.* **2012**, *66*, 628−635.



DOI: 10.1021/acs.analchem.5b00774
*Anal. Chem.* 2015, 87, 5056−5061